A&A 502, 391–394 (2009)
DOI: 10.1051/0004-6361/200912018

Astronomy & Astrophysics

The 0.5M_J transiting exoplanet WASP-13b⋆

I. Skillen[1,2], D. Pollacco[2], A. Collier Cameron[3], L. Hebb[3], E. Simpson[2], F. Bouchy[4,5], D. J. Christian[2,14], N. P. Gibson[2], G. Hébrard[4], Y. C. Joshi[2], B. Loeillet[12], B. Smalley[9], H. C. Stempels[3], R. A. Street[6], S. Udry[7], R. G. West[8], D. R. Anderson[9], S. C. C. Barros[2], B. Enoch[3], C. A. Haswell[10], C. Hellier[9], K. Horne[3], J. Irwin[11], F. P. Keenan[2], T. A. Lister[9,6], P. Maxted[9], M. Mayor[7], C. Moutou[12], A. J. Norton[10], N. Parley[10,3], D. Queloz[7], R. Ryans[2], I. Todd[2], P. J. Wheatley[13], and D. M. Wilson[9,15]

(Affiliations can be found after the references)

Received 9 March 2009 / Accepted 12 May 2009

ABSTRACT

We report the discovery of WASP-13b, a low-mass $M_p = 0.46^{+0.06}_{-0.05}\ M_J$ transiting exoplanet with an orbital period of 4.35298 ± 0.00004 days. The transit has a depth of 9 mmag, and although our follow-up photometry does not allow us to constrain the impact parameter well ($0 < b < 0.46$), with radius in the range $R_p \sim 1.06$–$1.21\ R_J$ the location of WASP-13b in the mass-radius plane is nevertheless consistent with H/He-dominated, irradiated, low core mass and core-free theoretical models. The G1V host star is similar to the Sun in mass ($M_* = 1.03^{+0.11}_{-0.09}\ M_\odot$) and metallicity ([M/H] = 0.0 ± 0.2), but is possibly older ($8.5^{+5.5}_{-4.9}$ Gyr).

Key words. binaries: eclipsing – planetary systems – techniques: photometric – techniques: radial velocities – techniques: spectroscopic – stars: individual: WASP-13b

1. Introduction

The discovery of transiting planets is a prominent theme in modern astrophysics. Even in the era of space-borne surveys such as CoRoT (Barge et al. 2007), the detection of a new transiting planet remains an important and celebrated discovery. In part this is because these are the only systems for which accurate physical parameters can be determined, which in turn enables their mass-radius relationship to be used as a diagnostic to constrain models of exoplanet structure and evolution. Currently there are some sixty transiting exoplanets known, and these manifest significant diversity in their physical properties.

There are four leading ground-based transit surveys: HATNet (Bakos et al. 2004), the Trans-Atlantic Exoplanet Survey (Dunham et al. 2004; O'Donovan et al. 2006), WASP Pollacco et al. (2006) and XO (McCullough et al. 2006). Each uses specialist instruments capable of imaging the sky over extremely large angular scales, and consequently are optimised to obtain high precision photometry for relatively bright stars. Early predictions were optimistic about the expected planetary yields (Horne 2003) in such wide-angle surveys. As a clearer understanding of the effects of systematic noise on the photometry has emerged (Pont et al. 2006; Smith et al. 2006), the discovery rates now broadly reflect these predictions. For example, the WASP survey announced the discovery of thirteen transiting exoplanets over the period August 2007 to April 2008. While space-based surveys are superior to ground-based ones for the detection of small planets and long-period systems, ground-based surveys are likely to remain important as their extremely large fields-of-view make them ideal for surveys of bright stars, which are well suited for detailed follow-up observations using other facilities.

In this paper we describe the discovery of a new, relatively low-mass exoplanet, WASP-13b, which was detected as part of the SuperWASP-North survey.

2. Observations and data reduction

The WASP Cameras are wide-field imaging facilities designed for the detection of exoplanetary transits. There are two similar facilities: SuperWASP-North (hereafter SuperWASP-N) on the island of La Palma in the Canary Islands, and WASP-South located at Sutherland, South Africa. The instrumentation and infrastructure used to obtain, store and reduce the data are described in detail in Pollacco et al. (2006). WASP-13 (= 1SWASP J092024.70+335256.6 = 2MASS J09202471+3352567 = USNO-B1.0 1238-0183620), a V = 10.51 G1V star in Lynx, was monitored with the SuperWASP-N Camera from 2006 November 27 to 2007 April 1, during which 3329 30-second images were obtained with a cadence of ∼7 mn. It was identified as a transit candidate using the algorithm outlined by Collier Cameron et al. (2007), and its lightcurve is shown in Fig. 1 (top panel).

Further R-band photometry was obtained with the 0.95 m James Gregory Telescope (JGT) located at St Andrews, Scotland, during the transit of 2008 February 16. The camera on this telescope consists of a 1024 × 1024 e2v CCD with an unvignetted field-of-view of 15′ in diameter. A total of 1047 15-second exposures was obtained in clear conditions with seeing of 4–5″ throughout the night. The last 20 images in the sequence were obtained under thick cloud cover and are not used in the final lightcurve. Data were processed using the *Cambridge Astronomical Survey Unit* data reduction and photometry pipeline (Irwin & Lewis 2001). Aperture photometry

⋆ The SuperWASP and JGT differential photometry, and SOPHIE radial velocities of WASP-13 are only available in electronic form at the CDS via anonymous ftp to `cdsarc.u-strasbg.fr (130.79.128.5)` or via `http://cdsweb.u-strasbg.fr/cgi-bin/qcat?J/A+A/502/391`

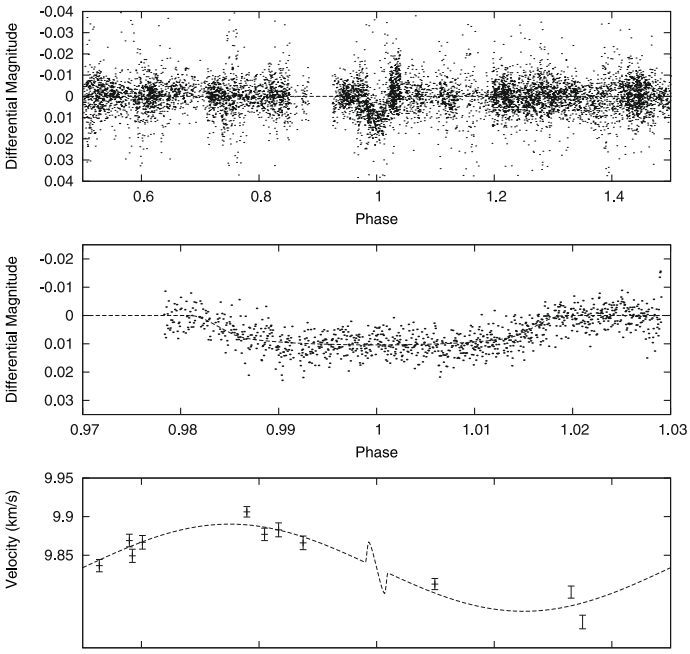

Fig. 1. Phased light and radial-velocity curves for WASP-13 obtained with SuperWASP-N (*top*), the JGT (*middle*) and SOPHIE (*bottom*). MCMC model solutions are shown as dotted lines for each data set, and the radial velocity model includes the predicted Rossiter-McLaughlin effect assuming the upper-limit $v \sin i$ (4.9 km s^{-1}).

with an 8″ radius aperture was performed on all stars in the field, and seven bright reference stars were selected for the differential photometry. The flux of the combined reference star is dominated by a single bright star, HD80408, situated 7.6′ from the target and approximately two magnitudes brighter. HD80408 ($V-K$ = 1.9) is within one spectral class of the planet host star ($V-K$ = 1.4).

The transit ingress was adversely affected by extinction because the data were obtained at high airmass in humid conditions. The data display a trend with airmass which we removed by subtracting a third-degree polynomial fit to the residuals from an initial model fit to the original differential light curve. There was essentially no correction to the measurements obtained at sec Z < 1.5, and the amplitude of the correction for 1.5 < sec Z < 1.8 ranges from 0.5 to 5 mmag. The adopted JGT lightcurve is shown in Fig. 1 (middle panel).

WASP-13 was observed with the Observatoire de Haute-Provence 1.93 m telescope and the SOPHIE stabilised spectrograph (Bouchy et al. 2006) during the period 2008 February 11–15, and eleven spectra were acquired with exposure time of 600-s and signal-to-noise ~40–60 measured in echelle order 26 at $\lambda \sim 550$ nm (SN26). We configured the instrument in its high efficiency mode with a resolution of R = 40 000, acquiring simultaneous star and sky spectra through separate fibres. Thorium-Argon calibration images were taken at the start and end of each night, and at 2- to 3-hourly intervals throughout each night. The radial-velocity drift never exceeded 2–3 m/s, even on a night-to-night basis. Spectra were reduced with the standard SOPHIE pipeline and corrections applied for lunar contamination of the cross-correlation function as needed.

A further three spectra of WASP-13 with resolution R = 46 000 were acquired with the 2.5 m Nordic Optical Telescope (NOT) using the FIES echelle spectrograph, with the aim of determining the host-star parameters (see Sect. 3.1). These spectra were extracted with the bespoke data reduction package, FIEStool.

Table 1. Log of SOPHIE observations of WASP-13.

BJD	Phase	$SN26$	RV (km s^{-1})	σ_{RV} (km s^{-1})	$V_{\rm span}$ (km s^{-1})
2454508.48441	0.875	45.7	9.8660	0.0088	0.020
2454509.45978	0.099	56.1	9.8126	0.0072	–0.005
2454510.46914	0.331	51.7	9.8022	0.0078	0.017
2454510.55389	0.350	45.3	9.7634	0.0088	0.007
2454511.32838	0.538	51.1	9.8365	0.0080	0.016
2454511.55075	0.579	50.1	9.8690	0.0082	0.009
2454511.57290	0.584	47.3	9.8492	0.0086	0.032
2454511.64730	0.602	46.6	9.8667	0.0088	–0.003
2454512.42051	0.779	60.9	9.9062	0.0068	0.028
2454512.55184	0.809	51.2	9.8770	0.0080	0.010
2454512.65565	0.833	45.0	9.8829	0.0090	–0.013

Table 2. Parameters of WASP-13.

RA = 09$^{\rm h}$20$^{\rm m}$24$^{\rm s}$.70,	Dec.= +33°52′56″.6
$T_{\rm eff}$	5826 ± 100 K
log g	4.04 ± 0.2
[M/H]	0.0 ± 0.2
log n(Li)	2.06 ± 0.1
$v \sin i$	<4.9 km s^{-1}
Spectral type	G1V
V mag	10.42
Distance	155 ± 18 pc

3. Results

The SuperWASP-N and JGT lightcurves show the presence of a 9 mmag dip of duration ~3.9 h which repeats with a period of ~4.35 days.

The radial velocities derived from the SOPHIE observations are listed in Table 1 and plotted in the lower panel of Fig. 1. WASP-13 exhibits radial-velocity variability in phase with that expected from reflex motion caused by a transiting exoplanet. We examined the line-bisector span, $V_{\rm span}$ (Table 1), in the manner described by Christian et al. (2009) to search for asymmetries in spectral line profiles that could result from unresolved binarity or indeed stellar activity. Such effects would cause the bisector spans to vary in phase with radial velocity, but no significant correlation is detected. We conclude that the observed photometric and radial-velocity variability is caused by an orbiting, planet-mass body.

3.1. Stellar and planetary parameters

We used the NOT echelle spectra to derive the host-star parameters (Table 2). Following procedures developed in our analyses of similar systems e.g. WASP-1 Stempels et al. (2007), we find $T_{\rm eff}$ = 5826 ± 100 K, log g = 4.04 ± 0.2 dex and [M/H] = 0.0±0.2 dex, which is consistent with solar metallicity. The effective temperature and near-solar mass (below) suggest a G1 spectral type. The host star has a detectable Li 6708 line from which we derive a lithium abundance log n(Li) = 2.06 ± 0.1 dex. The rotational line profile of WASP-13 is unresolved in the FIES spectra, and we derive an upper limit to $v \sin i$ of 4.9 km s^{-1} by subtracting in quadrature the macroturbulence appropriate to $T_{\rm eff}$ = 5826 K (4.1 km s^{-1}) from the instrumental profile (6.4 km s^{-1}).

Table 3. WASP-13 system parameters and their 1σ error limits.

Parameter	Symbol	$b = 0.46$	$b = 0.0$	Units
Transit epoch (BJD)	T_0	$2454491.6161^{+0.0007}_{-0.0007}$	$2454491.6161^{+0.0006}_{-0.0006}$	days
Orbital period	P	$4.35298^{+0.00004}_{-0.00004}$	$4.35298^{+0.00004}_{-0.00003}$	days
Planet/star area ratio	$(R_p/R_s)^2$	$0.0087^{+0.0004}_{-0.0004}$	$0.0082^{+0.0002}_{-0.0002}$	
Transit duration	t_T	$0.163^{+0.003}_{-0.003}$	$0.160^{+0.0015}_{-0.0015}$	days
Impact parameter	b	$0.46^{+0.13}_{-0.21}$	0 (adopted)	R_*
Eccentricity	e	0 (adopted)	0 (adopted)	
Stellar reflex velocity	K_1	$0.0557^{+0.0054}_{-0.0055}$	$0.0556^{+0.0055}_{-0.0054}$	km s^{-1}
Centre-of-mass velocity	γ	$9.8340^{+0.0015}_{-0.0014}$	$9.8340^{+0.0014}_{-0.0015}$	km s^{-1}
Orbital semimajor axis	a	$0.0527^{+0.0017}_{-0.0019}$	$0.0527^{+0.0018}_{-0.0020}$	AU
Orbital inclination	i	$86.9^{+1.6}_{-1.2}$	90.0	degrees
Stellar mass	M_*	$1.03^{+0.11}_{-0.09}$	$1.03^{+0.11}_{-0.11}$	$M_\odot$
Stellar radius	R_*	$1.34^{+0.13}_{-0.11}$	$1.20^{+0.04}_{-0.05}$	$R_\odot$
Stellar surface gravity	$\log g_*$	$4.19^{+0.07}_{-0.07}$	$4.29^{+0.02}_{-0.02}$	[cgs]
Stellar density	ρ_*	$0.43^{+0.12}_{-0.10}$	$0.60^{+0.02}_{-0.02}$	$\rho_\odot$
Planet radius	R_p	$1.21^{+0.14}_{-0.12}$	$1.06^{+0.05}_{-0.04}$	R_J
Planet mass	M_p	$0.46^{+0.06}_{-0.05}$	$0.45^{+0.05}_{-0.05}$	M_J
Planetary surface gravity	$\log g_p$	$2.85^{+0.10}_{-0.10}$	$3.02^{+0.04}_{-0.05}$	[cgs]
Planet density	ρ_p	$0.25^{+0.08}_{-0.08}$	$0.39^{+0.06}_{-0.06}$	ρ_J
Planet temperature ($A = 0$)	T_{eql}	1417^{+62}_{-58}	1339^{+6}_{-6}	K
Planet Safronov number	Θ	$0.039^{+0.008}_{-0.008}$	$0.043^{+0.007}_{-0.007}$	

In addition to the spectrum analysis we used photometry from Tycho, $V_T = 10.51$ and $(B - V)_T = 0.89$, and 2MASS, $(V_T - H) = 1.33$ and $(V_T - K) = 1.39$, to estimate the effective temperature using the Infrared Flux Method (Blackwell & Shallis 1977). This yields $T_{\rm eff} = 5935 \pm 183$ K, in close agreement with that obtained from the spectroscopic analysis. The Tycho and 2MASS colours suggest a spectral type of F9V (Collier Cameron et al. 2006).

The light and radial-velocity curves for WASP-13 were modelled simultaneously using the method described by Pollacco et al. (2008). The initial solution from the Monte-Carlo Markov Chain (MCMC) routine converged with a stellar density $\rho_* = 0.43^{+0.12}_{-0.10}\ \rho_\odot$. To determine the mass and age of WASP13 we compared its structure and effective temperature with the solar-metallicity stellar evolutionary models of Girardi et al. (2000). In Fig. 2 we plot the inverse cube root of the stellar density $\rho_*^{-1/3} = R_*/M_*^{1/3}$ (solar units) against effective temperature for the model mass tracks and isochrones, and for WASP13. We adopt this parameter space because $\rho_*^{-1/3}$ unlike R_* or luminosity, is measured directly from the light-curve and is independent of the effective temperature determined from the spectrum (Hebb et al. 2009). We interpolated the evolutionary tracks and isochrones in the $\rho_*^{-1/3} - T_{\rm eff}$ plane and find the mass of WASP13 to be $M_* = 1.03^{+0.11}_{-0.09}\ M_\odot$ and its age to be $8.5^{+5.5}_{-4.9}$ Gyr. Uncertainties in the derived stellar density, temperature and metallicity are included in the overall errors on the age and mass, but systematic errors due to differences between various evolutionary models are not. The large error in metallicity of ±0.2 dex contributes significantly to the uncertainty in the mass and age, and a more accurate spectral synthesis would improve the precision of these parameters. Nevertheless, we re-ran the transit fitting code a second and final time, adopting an initial value for the stellar mass of 1.03 $M_\odot$ and assuming a 10% uncertainty in this parameter. Our results are summarised in Table 3.

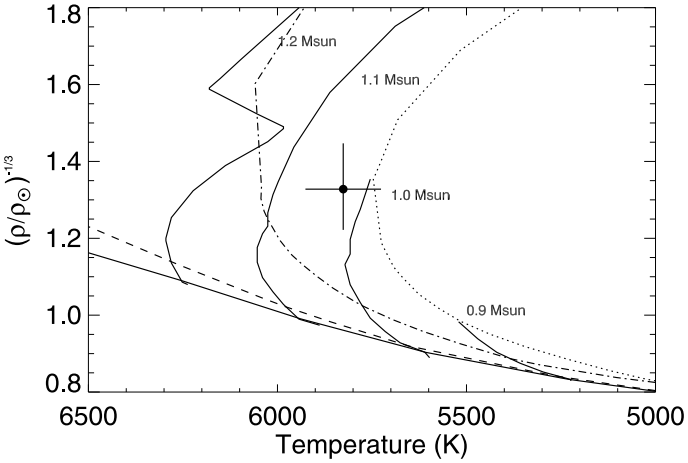

Fig. 2. Location of WASP-13 in the $(\rho/\rho_\odot)^{-1/3}$ vs. $T_{\rm eff}$ (K) plane compared to solar-metallicity stellar evolution mass tracks from Girardi et al. (2000). The mass tracks are labelled, and the isochrones are 0.1 Gyr, solid; 1 Gyr, dashed; 5 Gyr, dot-dashed; 10 Gyr, dotted. According to these models WASP-13 has a mass of $M_* = 1.03^{+0.11}_{-0.09}\ M_\odot$ and an age of $8.5^{+5.5}_{-4.9}$ Gyr.

The adopted solution yields an impact parameter $b = 0.46^{+0.12}_{-0.21}$, orbital inclination $i = 86.9^{+1.6}_{-1.2}$ degrees and transit duration $\tau = 0.163 \pm 0.003$ day, leading to a radius of $R_* = 1.34^{+0.13}_{-0.11}4\ R_\odot$ for the 1.03 $M_\odot$ host star. According to the stellar models, a solar metallicity star of this size and mass has evolved off the zero-age main sequence and is in the shell hydrogen burning phase of evolution with an age of 8.5 Gyr. The Li abundance measured in the spectral synthesis also suggests the star is several Gyr old, but it does not provide a precise age determination. The abundance is similar to, or slightly less than, levels found in open clusters with ages of 2–8 Gyr (Sestito & Randich 2005).

Our data suggests a large stellar radius and an old age for the host star. However, the JGT photometry does not constrain the impact parameter strongly. This affects the derived stellar radius and as a consequence, the derived age and planetary radius. Therefore, we also present a solution for the $b = 0$ case, which gives a lower limit to the stellar and planetary radii. We note that the χ^2 with respect to the $b = 0$ model fit is only marginally worse than the overall best fitting model. We encourage acquisition of higher quality photometry of this object to enable more accurate host-star and planet radii to be determined.

Although we provide only relatively weak constraints on the planet's radius, its mass is well constrained from the radial-velocity analysis. With $M_{\rm p} = 0.46^{+0.05}_{-0.06}\ M_J$, WASP-13b is amongst the lowest-mass transiting exoplanets, and with an inflated radius in the range $R_{\rm p} \sim 1.06{-}1.21\ R_{\rm J}$ its position in the mass-radius plane is broadly consistent with the H/He-dominated, low core mass and core-free irradiated models of Fortney et al. (2007).

The Safronov number for WASP-13b is $\Theta = 0.039 \pm 0.008$ for the $b = 0.46$ case, and $\Theta = 0.043 \pm 0.007$ for the $b = 0$ case. This places it amongst the hotter, less-massive Class II giant exoplanets in the classification scheme of Hansen & Barman (2007), who proposed that transiting exoplanets can be distinguised into two classes according to their equilibrium temperatures and Safronov numbers. Recently, Torres et al. (2008) reported additional support of this dichotomy. However, Fressin et al. (2009) suggested on the basis of simulations of a model population of stars and exoplanets that the apparent grouping into distinct classes is not statistically significant. A bimodal distribution of Safronov number for giant exoplanets would have implications for models of their formation and evolutionary history. Continued discovery and parametrization of new transiting exoplanets is needed to confirm this hypothesis.

Acknowledgements. The WASP Consortium comprises astronomers primarily from the Universities of Keele, Leicester, The Open University, Queen's University Belfast, the University of St Andrews, the Isaac Newton Group (La Palma), the Instituto de Astrofísica de Canarias (Tenerife) and the South African Astronomical Observatory. The SuperWASP-N camera is hosted by the Isaac Newton Group on La Palma with funding from the UK Science and Technology Facilities Council. We extend our thanks to the Director and staff of the Isaac Newton Group for their support of SuperWASP-N operations. F.P.K. would like to acknowledge A.W.E., Aldermaston for the award of a William Penney Fellowship.

Based in part on observations made at Observatoire de Haute Provence (CNRS), France, and on observations made with the Nordic Optical Telescope, operated on the island of La Palma jointly by Denmark, Finland, Iceland, Norway, and Sweden, in the Spanish Observatorio del Roque de los Muchachos of the Instituto de Astrofisica de Canarias.

References

Bakos, G., Noyes, R. W., Kovács, G., et al. 2004, PASP, 116, 266
Barge, P., Baglin, A., Auvergne, M., & The CoRoT Team 2007, in EXOPLANETS: Detection, Formation and Dynamics, Proc. IAU Symp., 249
Blackwell, D. E., & Shallis, M. J. 1977, MNRAS, 180, 177
Bouchy, F., The Sophie Team 2006, in Tenth Anniversary of 51 Peg-b: Status of and prospects for hot Jupiter studies, ed. L. Arnold, F. Bouchy, & C. Moutou, 319
Christian, D. J., Gibson, N. P., Simpson, E., et al. 2009, MNRAS, 392, 1585
Collier Cameron, A., Pollacco, D., Street, R. A., et al. 2006, MNRAS, 373, 799
Collier Cameron, A., Wilson, D. M., West, R. G., et al. 2007, MNRAS, 380, 1230
Dunham, E. W., Mandushev, G. I., Taylor, B. W., & Oetiker, B. 2004, PASP, 116, 1072
Fortney, J. J., Marley, M. S., & Barnes, J. W. 2007, ApJ, 659, 1661
Fressin, F., Guillot, T., & Nesta, L. 2009 [arXiv:0901.3083]
Girardi, L., Bressan, A., Bertelli, G., & Chiosi, C. 2000, A&AS, 141, 371
Hansen, B. M. S., & Barman, T. 2007, ApJ, 671, 861
Hebb, L., Collier-Cameron, A., Loeillet, B., et al. 2009, ApJ, 693 1920
Horne, K. D. 2003, Scientific Frontiers of Exoplanet Research, ed. Deming & Seager (San Francisco), ASP Conf., 294, 361,
Irwin, M., & Lewis, J. 2001, NewAR, 45, 105
McCullough, P. R. 2006, ApJ, 648, 1228
O'Donovan, F. T., Charbonneau, D., Torres, G., et al. 2006, ApJ, 644, 1237
Pollacco, D. L., Skillen, I., Cameron, A. Collier, et al. 2006, PASP, 118, 1407
Pollacco, D., Skillen, I., Collier Cameron, A., et al. 2008, MNRAS, 385, 1576
Pont F., Zucker, S. & Queloz, D. 2006, MNRAS, 373, 231
Sestito, P., & Randich, S. 2005, A&A, 442, 615
Smith, A. M. S., Collier Cameron, A., Christian, D. J., et al. 2006, MNRAS, 373, 1151
Stempels, H. C., Collier Cameron, A., Hebb, L., Smalley, B., & Frandsen, S. 2007, MNRAS, 379, 773
Torres, G., Winn, J. N., & Holman, J. 2008, ApJ, 677, 1324

[1] Isaac Newton Group of Telescopes, Apartado de Correos 321, 38700 Santa Cruz de la Palma, Tenerife, Spain
e-mail: wji@ing.iac.es
[2] Astrophysics Research Centre, School of Mathematics & Physics, Queen's University, University Road, Belfast, BT7 1NN, UK
[3] School of Physics and Astronomy, University of St Andrews, North Haugh, St Andrews, Fife KY16 9SS, UK
[4] Institut d'Astrophysique de Paris, CNRS (UMR 7095) – Université Pierre & Marie Curie, 98$^{\rm bis}$ bvd. Arago, 75014 Paris, France
[5] Observatoire de Haute-Provence, 04870 St Michel l'Observatoire, France
[6] Las Cumbres Observatory, 6740 Cortona Dr. Suite 102, Santa Barbara, CA 93117, USA
[7] Observatoire de Genève, Université de Genève, 51 Ch. des Maillettes, 1290 Sauverny, Switzerland
[8] Department of Physics and Astronomy, University of Leicester, Leicester, LE1 7RH, UK
[9] Astrophysics Group, Keele University, Staffordshire, ST5 5BG, UK
[10] Department of Physics and Astronomy, The Open University, Milton Keynes, MK7 6AA, UK
[11] Institute of Astronomy, University of Cambridge, Madingley Road, Cambridge, CB3 0HA, UK
[12] Laboratoire d'Astrophysique de Marseille, BP 8, 13376 Marseille Cedex 12, France
[13] Department of Physics, University of Warwick, Coventry CV4 7AL, UK
[14] Department of Physics and Astronomy, California State University, 18111 Nordhoff Street, Northridge, CA, USA
[15] Centre for Astrophysics and Planetary Science, School of Physical Sciences, University of Kent, Canterbury, Kent, CT2 7NH, UK